

Synthesis and Melt Dynamics of Model Sulfonated Ionomers

Neena K. Tierney^{†,§} and Richard A. Register^{*,†,‡}*Department of Chemical Engineering and Princeton Materials Institute, Princeton University, Princeton, New Jersey 08544**Received November 22, 2002; Revised Manuscript Received December 30, 2002*

ABSTRACT: We investigate the dynamics of model ionomers through linear viscoelastic measurements on well-defined sulfonated styrene–ethylene–butene (SEB) ionomers of varying molecular weights and functionalization levels. Random styrene–butadiene copolymers with low polydispersities were synthesized via anionic polymerization, from which ionomers were prepared by selective hydrogenation of the butadiene units, followed by partial sulfonation of the styrene units and subsequent neutralization. The low glass transition temperature of the SEB backbone provides access to both the rubbery and terminal flow regions in lightly functionalized materials. All ionomers show multiple relaxation mechanisms and do not obey time–temperature superposition. We identify the faster relaxations with motions of the outermost portions of the polymer chains, which contain no ionic groups. Rapid relaxation of these chain segments leads to a plateau modulus for the ionomers lower than that for highly entangled unfunctionalized SEB, despite the ionic associations. The slower relaxations correspond to the ion-hopping process and to the terminal relaxation time of the polymer chain; these two relaxations overlap for the low number of ionic groups per chain explored. The terminal relaxation time shows only a weak dependence on molecular weight but an extremely strong dependence on sulfonation level, reflecting a strong dependence of the ion-hopping time on the extent of functionalization.

Introduction

Ionomers are polymers that contain a small amount of covalently bound ionic functionality, typically distributed randomly along a high molecular weight backbone. Ionomer melt flow behavior is dramatically affected by aggregation of these ionic groups, yielding viscosities and terminal relaxation times that are orders of magnitude greater than comparable nonionic polymers.¹ It is postulated^{1,2} that there are two important relaxation processes occurring in ionomers: the terminal relaxation time of the polymer chains, t_d , and the average lifetime of an ionic association, τ . The latter is the average length of time an ionic group spends in a particular aggregate before it “hops” to another aggregate, thus allowing relaxation of the polymer chain segment attached to the ionic group.^{3,4} The terminal relaxation time, t_d , of the ionomer is increased due to the slowed motion of the polymer chains caused by these temporary ionic cross-links.

Systematic studies of the flow behavior of ionomers are hampered by the nonideal molecular architectures which they typically present. Most commonly, ionomers are prepared by free-radical copolymerization of a nonionic monomer and an acidic (or ionic) comonomer, yielding a substantial chain length polydispersity. Moreover, it is difficult to precisely match the chain length average and distribution between two independently synthesized copolymers, complicating a direct assessment of the effect of ion content. Furthermore, chain transfer to polymer can introduce long-chain branching, which substantially impacts the rheology; ethylene–co-methacrylic acid (E/MAA) ionomers, which are impor-

tant commercial products, possess substantial long-chain branching.^{5,6}

These complications underscore the value of a model system for the study of ionomer dynamics, beginning with the simplest case of linear, near-monodisperse chains. Ideally, the ionic groups would be introduced by mild post-polymerization functionalization, such that ionomers of different ion content can be prepared from a single unfunctionalized precursor, without any side reactions that alter the chain length or distribution. Sulfonated polystyrene is well-established as a model ionomer; styrene may be polymerized anionically to yield a near-monodisperse product, which may be subsequently reacted to introduce sulfonate groups randomly along the chain at any moderate level.⁷ Indeed, the melt dynamics of such near-monodisperse sulfonated polystyrene ionomers have been described by Colby and co-workers in a brief report.² However, the high glass transition temperature of polystyrene (ca. 100 °C), coupled with the limited thermal stability of sulfonated ionomers based on hydrocarbon polymers, leads to a rather narrow temperature range over which melt rheological measurements can be made, hindering critical tests of time–temperature superposition. These temperature limitations also restrict the ranges of molecular weight and functionalization level over which terminal flow can be accessed, yet terminal measurements are particularly desired for comparison with theoretical predictions, such as the scaling of terminal relaxation time with chain length and ionic group content.^{2,8}

Here, we present the synthesis and rheological characterization of a family of sulfonated styrene–ethylene–butene (SEB) random terpolymers. The backbones of these polymers are synthesized via anionic polymerization, yielding the desired narrow molecular weight distribution and linear architecture. Ionic groups are introduced by the same post-polymerization functionalization route used for SPS. However, unlike SPS,

* To whom correspondence should be addressed: e-mail register@princeton.edu.

[†] Department of Chemical Engineering.

[‡] Princeton Materials Institute.

[§] Present address: Johnson & Johnson Consumer Products Worldwide, Skillman, NJ 08558.

these sulfonated SEB ionomers have a glass transition temperature of approximately $-15\text{ }^{\circ}\text{C}$, greatly expanding the window over which melt rheological measurements can be made. These sulfonated SEB materials thus provide access to both the rubbery and terminal flow regions for ionomers of known and well-controlled structure, permitting a systematic investigation of the dynamics in both regions.

Experimental Section

Polymerization. Standard methods of vacuum anionic polymerization were employed. *n*-Butyllithium (*n*BuLi) initiator was charged to the flamed reactor in a glovebox, along with *N,N,N',N'*-tetramethylethylenediamine (TMEDA), previously distilled from dibutylmagnesium (Bu_2Mg), in a 4:1 TMEDA:Li ratio, to randomize the styrene–butadiene sequence.^{9,10} Solvents and monomers were charged to the reactor volumetrically via vacuum transfer from a suitable drying agent (Bu_2Mg for styrene, 0.909 g/cm^3 at $23\text{ }^{\circ}\text{C}$; *n*BuLi for butadiene, 0.64 g/cm^3 at $0\text{ }^{\circ}\text{C}$; diphenylhexyllithium for cyclohexane). The monomer composition was targeted at 40 wt % styrene for all polymerizations; initial monomer contents in the cyclohexane reaction mixture were 10–20 wt %. The polymerizations were run at $50\text{ }^{\circ}\text{C}$, and all exhibited the characteristic orange-red color of the polystyryl end in the presence of TMEDA. Polymerizations were terminated after 60 min by the addition of degassed 2-propanol.

Hydrogenation. Selective saturation of the butadiene units was achieved with a soluble Ni/Al catalyst, following procedures previously described.^{11,12} Saturations were carried out at $80\text{ }^{\circ}\text{C}$, under 400 psi of H_2 , with the polymer in cyclohexane solution at 1.5 wt %. Saturations were continued until no olefinic unsaturation was detectable by FTIR; in some cases, additional catalyst was charged to the reactor, and saturation was typically complete within 24 h. Catalyst residue was subsequently removed from the polymer solution by vigorously stirring with aqueous citric acid (16 wt %). Storey et al. have observed that the polymers can darken during the subsequent sulfonation reaction if not free of catalyst residue.¹³

Sulfonation and Neutralization. Acetyl sulfate was used to randomly sulfonate a minor fraction of the styrene groups.⁷ Typically, the polymer was dissolved at 10 wt % in an 80/20 mixture of 1,2-dichloroethane/cyclohexane and sparged with nitrogen for 30 min. A solution of 1.0 M acetyl sulfate was prepared in situ in 1,2-dichloroethane at $0\text{ }^{\circ}\text{C}$ by adding the requisite quantities of sulfuric acid (EM Science, 95%) and acetic anhydride (EM Science, 97%); a 50% molar excess of acetic anhydride was employed to scavenge trace water. Previous work from our laboratory¹⁴ indicated a sulfonation efficiency (based on sulfuric acid, the limiting reagent) for homopolystyrene of 74% under similar conditions. With this estimate of the efficiency, the necessary quantity of acetyl sulfate solution was added to the polymer solution at $50\text{ }^{\circ}\text{C}$. The reaction was allowed to proceed at $50\text{ }^{\circ}\text{C}$ for 2 h and then terminated with 2-propanol added in stoichiometric excess over the acetic anhydride. The polymer was isolated by pouring the solution into boiling deionized water. To remove any residual unreacted acid, the polymer crumbs were stirred in deionized water for 24 h, changing the water every 4 h. Successful sulfonation of the SEB terpolymers was evident by a small peak at 7.6–7.8 ppm in the ^1H NMR spectrum. Fully neutralized Na^+ ionomers were generated from the SSEB materials by titration to the phenolphthalein end point with NaOH in tetrahydrofuran (THF). These Na^+ SSEB ionomers were then analyzed for sulfur content (Galbraith Laboratories, Knoxville, TN) to determine the fraction of styrene units sulfonated. The sulfonation efficiency for the eight SSEB acid copolymers was found to be $72 \pm 6\%$, consistent with our initial estimate. The sulfur contents determined from elemental analysis were then used to calculate the charges of neutralizing agent required for fully neutralized Li^+ (using LiOH) and tributylammonium (TBA^+ , using tributylamine) salts of the SSEB acid materials, again in THF solution.

Table 1. Molecular Characteristics of Random Styrene–Butadiene (SBR) Copolymers

polymer	composition (wt %)			polydispersity index	M_w (kg/mol)
	S	1,4-B	1,2-B		
SBR16	39	27	34	1.06	15.6
SBR28	39	28	33	1.06	27.9
SBR46	41	26	33	1.05	45.9
SBR144	39	26	35	1.09	144

Polymer Characterization. Room temperature ^1H NMR spectra were recorded in *d*-dioxane (SBR copolymers) or *d*-chloroform (SEB terpolymers and sulfonated SSEB acids), using a GE QE-300 spectrometer. FTIR spectra of thin films cast onto NaCl plates were obtained using a Nicolet 730. Polydispersities and apparent molecular weights were obtained for the SBR copolymers and SEB terpolymers via gel permeation chromatography (GPC) in toluene at $35\text{ }^{\circ}\text{C}$, using refractive index detection (Waters 410) and two 30 cm PLgel Mixed-C columns (Polymer Laboratories), calibrated with narrow-distribution polystyrene standards. True weight-average molecular weights (M_w) were determined for the SBR copolymers at $25\text{ }^{\circ}\text{C}$ via light scattering (Light Scattering Instruments) at 632.8 nm and angles of $30\text{--}162\text{ }^{\circ}$, analyzed through the standard Zimm method. The refractive index increment at 632.8 nm of SBR copolymers of this composition and microstructure, in cyclohexane at $25\text{ }^{\circ}\text{C}$, was found to be $0.127\text{ cm}^3/\text{g}$ (measured on an LDC Analytical KMX-16). Differential scanning calorimetry (DSC) was employed to measure the glass transition temperatures (T_g) of the SEB terpolymers, using a Perkin-Elmer DSC-7 at a scanning rate of $10\text{ }^{\circ}\text{C}/\text{min}$, calibrated with indium and mercury.

Rheological Measurements. Disk specimens (28 mm diameter, 2 mm thick) were prepared under vacuum in a closed mold at $50\text{--}100\text{ }^{\circ}\text{C}$. Dynamic shear measurements were conducted using a Rheometrics mechanical spectrometer (RMS-800) with 25 mm parallel plate fixtures, at $10^{-3}\text{--}10^2\text{ rad/s}$ and $15\text{--}180\text{ }^{\circ}\text{C}$. The gap between the plates was 1–2 mm, and the strain amplitude was 0.5–5%, corresponding to the linear viscoelastic regime.

Cation Diffusion Measurements. A trilayer sandwich was prepared consisting of a thin layer of Na^+ -neutralized SSEB ionomer between two thicker layers of the same SSEB neutralized with Li^+ . The sandwich was annealed for 87 h at $120\text{ }^{\circ}\text{C}$ to permit interdiffusion and then cut in cross section and faced by ultramicrotomy. The resultant Na concentration profile was measured via X-ray microanalysis using a scanning electron microscope (FEI/Philips XL30) fitted with an energy-dispersive X-ray detector. Details of the specimen preparation and analysis methods have been described in detail elsewhere.⁶

Results and Discussion

A. Synthesis and Characterization. The sulfonated styrene–ethylene–butene (SEB) ionomers are prepared from an anionically polymerized random styrene–butadiene copolymer (SBR), which is hydrogenated to SEB, sulfonated, and neutralized. Anionic polymerization provides the desired linear architecture and narrow molecular weight distribution. To randomize the addition of styrene and butadiene units to the growing chain, *N,N,N',N'*-tetramethylethylenediamine (TMEDA) was added in a 4:1 TMEDA:Li molar ratio. Halasa and co-workers have demonstrated^{9,10} that TMEDA (at 2:1 TMEDA:Li or higher) effectively randomizes the chain sequence, confirmed here by synthesizing an analogous SBR containing 70 wt % styrene, degrading this with ozone, and analyzing the residue by liquid chromatography.¹⁵ TMEDA also substantially elevates the 1,2-enchainment of butadiene to greater than 50%. Table 1 lists the molecular characteristics of the four SBR copolymers synthesized in this work. All polymers contain $40 \pm 1\text{ wt } \%$ styrene, all have similar diene

Table 2. Na⁺-Neutralized Sulfonated Ionomers Prepared from SEB Terpolymers

sample notation	precursor SEB M_w (kg/mol)	mole fraction of styrene units sulfonated	av no. of ionic groups per chain (\bar{n})
Na16-3	16.0	0.056	3.3
Na16-4	16.0	0.077	4.5
Na16-5	16.0	0.085	4.9
Na28-4	28.5	0.040	4.1
Na28-6	28.5	0.054	5.6
Na28-7	28.5	0.070	7.3
Na28-10	28.5	0.095	9.9
Na47-9	46.9	0.052	9.4

microstructures, and all have polydispersity indices less than 1.1. Comparison of the true M_w values obtained by light scattering with the apparent (polystyrene-equivalent) values of M_w obtained by GPC yielded a consistent hydrodynamic equivalence ratio¹⁶ $r_B = 1.20$ in toluene at 35 °C.

Hydrogenation of the SBR to SEB prior to sulfonation is essential, as acetyl sulfate will react with any remaining 1,4-butadiene units to cleave the polymer chain. The Ni/Al catalyst employed can exhaustively saturate the 1,4- and 1,2-butadiene units while leaving the aromatic nuclei on the styrene units untouched^{11,12} and thus available for subsequent sulfonation. The *trans*-1,4-butadiene stretch at 968 cm⁻¹ is well-resolved and has a high extinction coefficient; we estimate that residual unsaturation at the level of 1 such unit per 100 000 g/mol of SEB terpolymer would be detectable by FTIR. All our polymers were saturated to below this detection limit to minimize potential chain scission during sulfonation. Since the SEB terpolymers contain less than 30 wt % 1,4-butadiene units and these units are randomly distributed, the SEB terpolymers show no crystallinity by DSC. Rather, each SEB terpolymer shows a single sharp glass transition centered at -15 °C (T_g). This low T_g opens a wide window for rheological measurements, since substantial degradation of the sulfonate groups does not occur until above 180 °C. The unfunctionalized SEB terpolymers are denoted below as SEBxx, where xx is the M_w value for the SEB terpolymer in kg/mol; this value was calculated from the M_w value for the corresponding SBR precursor by simply adding 2 H per butadiene unit, as GPC on the SEB terpolymers confirmed that no backbone rearrangements occurred during hydrogenation.¹⁷

Table 2 displays the characteristics of the Na⁺-neutralized sulfonated ionomers, each denoted as Na xx - \bar{n} , where xx is again the M_w value for the parent SEB terpolymer in kg/mol and \bar{n} is the average number of sodium sulfonate groups per chain, based on M_w . The quantities given in Table 2 are the same for the Li⁺ and TBA⁺ ionomers as for their Na⁺ counterparts, as all are fully neutralized; these other ionomers are denoted below by replacing "Na" in the sample code with "Li" or "TBA".

B. Melt Rheology. 1. Unfunctionalized SEB Terpolymers. Parts a and b of Figure 1 show storage (G') and loss (G'') modulus master curves at a reference temperature of 30 °C for the four SEB terpolymers. All four terpolymers follow time-temperature superposition closely, and the transition in G' from the rubbery plateau to the terminal zone is relatively sharp, as expected for unbranched entangled chains of narrow molecular weight distribution. For SEB147 at 10 rad/s (where the slope of G' vs frequency is a minimum), $G' = 7.8 \times 10^5$ Pa, which may be taken as the value of the

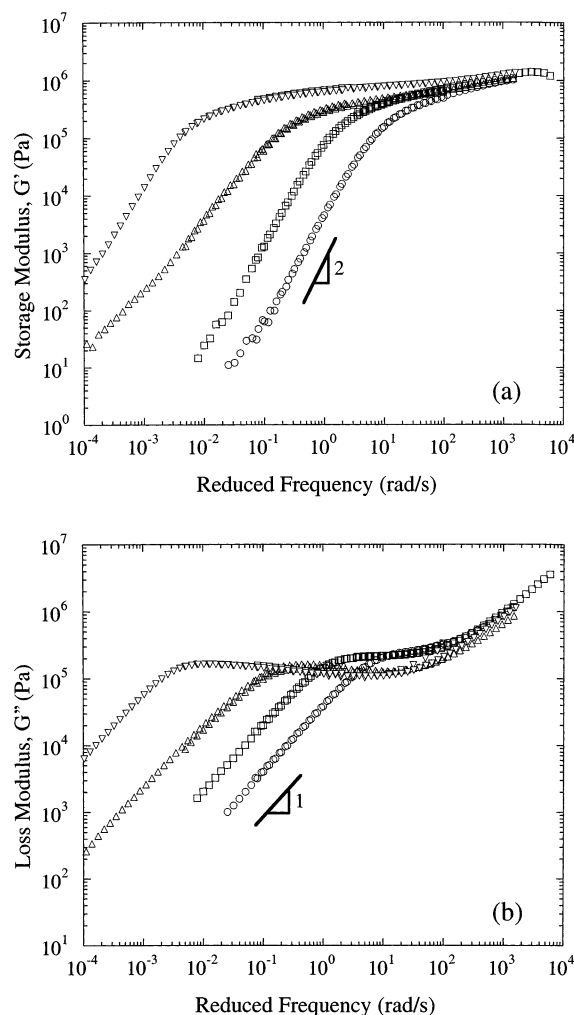


Figure 1. Storage modulus (G' , panel a) and loss modulus (G'' , panel b) master curves for unfunctionalized SEB terpolymers at a reference temperature of 30 °C: SEB16 (○), SEB28 (□), SEB47 (△), and SEB147 (▽).

plateau modulus G_N^0 for SEB terpolymers of this composition. This value of G_N^0 translates to an entanglement molecular weight (M_e) of approximately 2800 g/mol, following¹⁸ $M_e = \rho RT/G_N^0$, where ρ is the density at 30 °C ($\rho \approx 0.88$ g/cm³, calculated as the weighted average of the density of polystyrene in the melt extrapolated to room temperature¹⁹ and the density of hydrogenated polybutadiene (52% 1,2) with known thermal expansion coefficient²⁰).

2. Sulfonated SEB Ionomers. Before investigating the rheological behavior of the sulfonated ionomers, it is important to confirm that the sulfonation reaction does not induce any substantial backbone rearrangements. Unfortunately, GPC is not well-suited to this task, as associations between the sulfonate groups and the GPC packing can distort the chromatogram.²¹ However, for sulfonated polystyrene ionomers, Weiss and co-workers have shown^{22,23} that neutralization with a bulky organic counterion such as tributylammonium (TBA⁺) yields viscosities similar to those of the unfunctionalized polystyrene precursor, as the ionic groups interact only weakly. Figure 2 compares the complex viscosity η^* for SEB16 and TBA16-4, its tributylammonium sulfonate ionomer derivative. The ionomer has a zero-shear viscosity only 3 times that of its nonionic precursor, likely reflecting weak but real associations

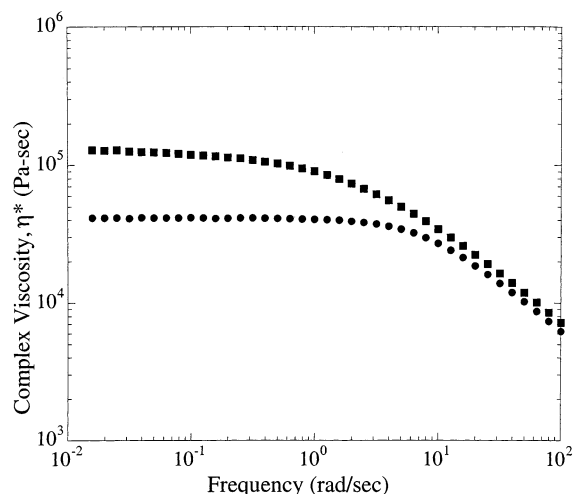


Figure 2. Complex viscosity (η^*) curves at 30 °C for the unfunctionalized SEB16 terpolymer (●) and for the TBA16-4 ionomer (■), where each sulfonate anion is paired with a tributylammonium (TBA^+) cation.

between tributylammonium sulfonate groups; this may be compared with a factor of 10^6 increase in η^* for Na16-5 over SEB16 (data presented below), which clearly rules out major backbone rearrangements as responsible for the pronounced rheological changes we find below in the sodium sulfonate derivatives.

While the unfunctionalized SEB16 exhibits terminal flow at 30 °C (Figure 2), its sodium sulfonate derivative Na16-5 does not show a transition to flow over the accessible frequency range until 90 °C is reached. To compare ionomers of varying functionalization level, where the terminal relaxation time may range over several orders of magnitude, we attempted to construct master curves using time–temperature superposition (TTS). Figure 3 shows G' and G'' “master” curves at a reference temperature of 120 °C for the Na16 (Figure 3a) and Na28 ionomers (Figure 3b). These pseudomaster curves were constructed by shifting the data horizontally to produce the best visual overlap; no vertical shifting was applied. For ionomers based on a single SEB terpolymer, the shift factors a_T were found to be similar, so a single set of a_T values (averaged) was used for the Na16 ionomers and a different (though similar) single set for the Na28 ionomers. Figure 3a shows that the terminal response of Na16-5 is shifted approximately 6 decades lower in frequency relative to SEB16, meaning that an average of 4.9 sulfonate groups per chain is sufficient to increase t_d by 6 orders of magnitude. (For the unfunctionalized unfunctionalized SEB16 at 120 °C, $t_d^0 \approx 5 \times 10^{-5}$ s, based on¹⁸ $t_d^0 = \eta_0 J_e^0$ and a recoverable compliance $J_e^0 = 3 \times 10^{-6}$ Pa⁻¹ measured via creep-and-recovery experiments¹⁷ on SEB28.) That such a large increase in t_d is achieved with such a modest number of ionic groups per chain indicates that the ionic association lifetime, τ , is fairly long (here, $\tau > t_d^0$). Moreover, because \bar{n} is small, the terminal relaxation at t_d is not well-separated from τ .

However, the poor superposition of different data segments evident in Figure 3 makes it clear that these ionomers do *not* follow TTS; that is, there is *no* set of shift factors a_T which can satisfactorily collapse the data taken at different temperatures. The breakdown of TTS indicates that multiple relaxation mechanisms are present in this time–temperature window and that these mechanisms do not have the same dependence

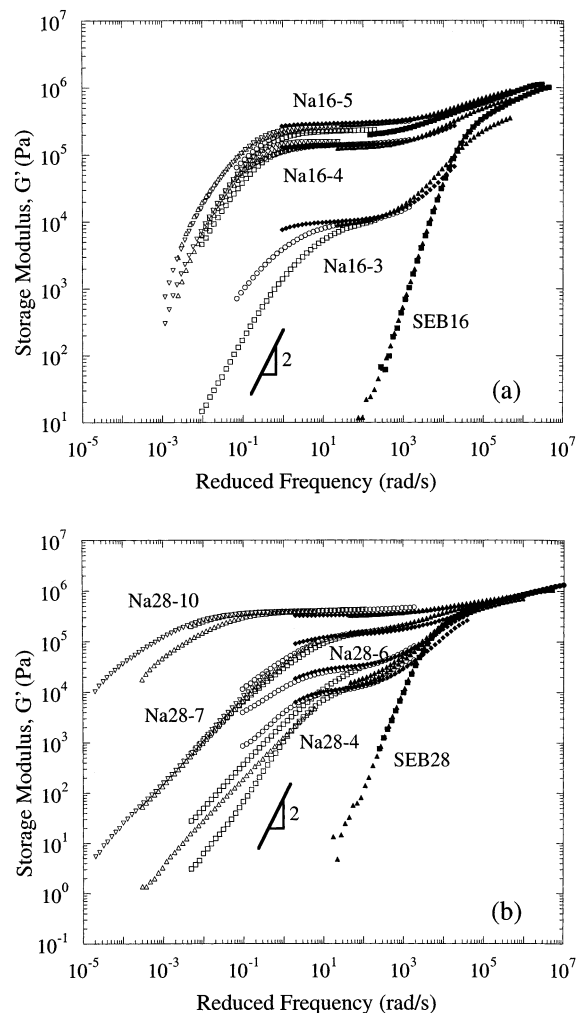


Figure 3. Storage modulus (G') pseudomaster curves at a reference temperature of 120 °C, constructed through common sets of a_T values for ionomers derived from a single parent SEB (see text; unfunctionalized SEB terpolymers use different sets of a_T than ionomers). (a) SEB16, Na16-3, Na16-4, and Na16-5. (b) SEB28, Na28-4, Na28-6, Na28-7, and Na28-10. Symbols shown in pseudomaster curves correspond to temperatures at which measurements were taken: 0 (●), 15 (■), 30 (▲), 60 (◆), 90 (○), 120 (□), 150 (△), and 180 °C (▽).

upon temperature. This contrasts with current theories of ionomer dynamics, where the only relaxation mechanisms considered are ion-hopping (time τ) and whole-chain relaxation of the ionomer (terminal time t_d), since t_d and τ are predicted to be related through a temperature-independent proportionality.^{2,8} Indeed, there are several prior reports of the failure of TTS in ionomers (reviewed in ref 1), including E/MAA salts²⁴ and styrene-based ionomers.²⁵ The lack of time–temperature superposition in those cases may reasonably be attributed to slightly different activation energies for the ion-hopping and terminal processes.¹ However, the departures from TTS observed there are generally not dramatic: viscoelastic curves acquired at different temperatures have similar shapes, with differences only evident when the curves are overlaid. Moreover, while other E/MAA^{6,26} and styrene-based ionomers²⁷ have been reported to obey TTS to within experimental error, it is plausible that these materials would also show a lack of superposition if data could be acquired over a broader range of time (or frequency) at each temperature.¹ By contrast, many of the curve segments in Figure 3 (corresponding

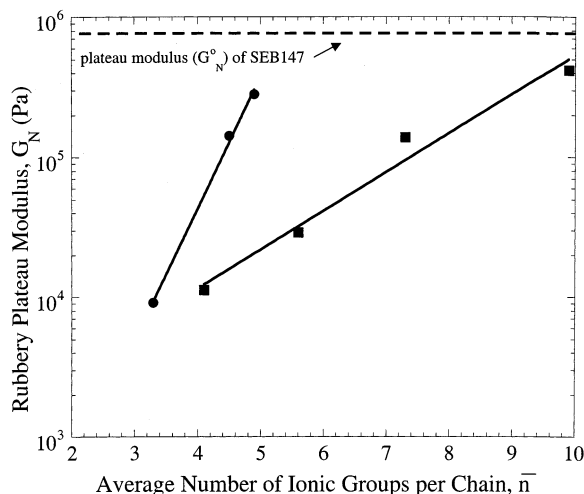


Figure 4. Rubbery plateau modulus (G_N) at 90 °C as a function of the average number of ionic groups per chain, \bar{n} , for ionomers derived from SEB16 (●) and SEB28 (■). Solid lines represent best exponential fits, while dashed horizontal line is the plateau modulus at 30 °C for a high-molecular-weight, nonionic SEB terpolymer of this composition. (A lower temperature, 30 vs 90 °C, is required for the terpolymer to exhibit a rubbery plateau.)

to different temperatures) have *distinctly* different shapes over comparable ranges of reduced frequency. This suggests that the severe breakdown of TTS for our sulfonated SSEB ionomers reflects not simply different activation energies for the ion-hopping and terminal processes, but the presence of an additional relaxation mechanism (with a different activation energy). Thus, an essential task is to identify the relaxation mechanisms present in our measurement window.

Close scrutiny of the ionomers' rubbery plateau moduli (G_N) provides valuable insight on this point. G_N was obtained as G' at the frequency where the slope of G' vs frequency is a minimum; the 90 °C data segment was used for each ionomer, as all show a rubbery plateau at this temperature. Figure 4 shows the expected increase in G_N with sulfonation level, expressed here as the average number of ionic groups per chain, \bar{n} . However, the plateau moduli for the ionomers all lie *below* the plateau modulus of the unfunctionalized, high molecular weight SEB147 (7.8×10^5 Pa), though they approach this value with increasing \bar{n} . This is contrary to our naive expectation: since the ionomers contain both entanglements and ionic associations, the ionomers should all show *higher* plateau moduli than SEB147. Indeed, this expectation is borne out in the data of Weiss et al.²⁷ for SPS ionomers, all of which have higher G_N values than nonionic polystyrene—but all of which have much larger values of \bar{n} than we explore here.

We rationalize this apparent contradiction by noting that, at the small values of \bar{n} characteristic of the ionomers in Figure 4, the “end sections” of each chain constitute a substantial fraction of the total chain length. Here, an “end section” is measured by starting at the chain end and working inward until the first ionic group is encountered. Since the end sections contain no ionic groups, they can relax rapidly even when they amount to a few M_e , if the ion-hopping time τ is relatively long—comparable to or longer than t_d^0 . Relaxation of the end sections will “dilute” the entanglement network, as has been thoroughly demonstrated for star and branched polymers by McLeish and Milner.^{28,29}

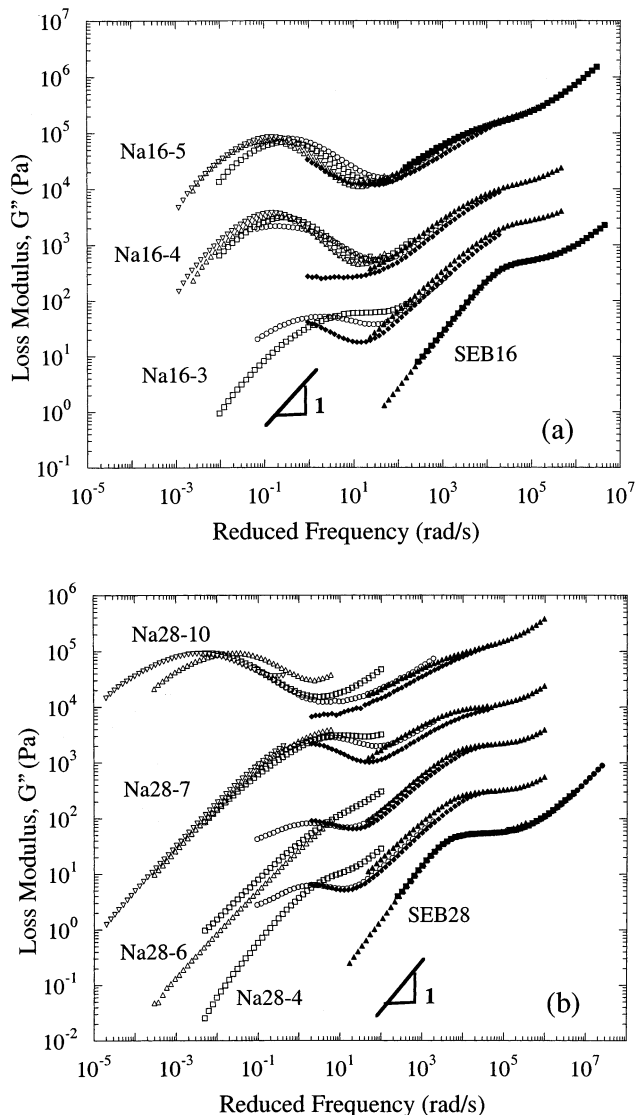


Figure 5. Loss modulus (G'') pseudomaster curves at 120 °C, corresponding to G' curves of Figure 3, and constructed with the same shift factors. The G'' data for the most highly functionalized ionomer in each panel are unshifted; the other curves are shifted downward by factors (given below) decreasing progressively with ion content, for clarity. (a) Na16-5, Na16-4 ($15\times$ downward shift in G''), Na16-3 ($50\times$), and SEB16 ($500\times$). (b) Na28-10, Na28-7 ($15\times$), Na28-6 ($100\times$), Na28-4 ($600\times$), and SEB28 ($4000\times$). Symbols shown in master curves correspond to temperatures at which measurements were taken: 0 (●), 15 (■), 30 (▲), 60 (◆), 90 (○), 120 (□), 150 (△), and 180 °C (▽).

Since the fraction of the chain constituted by these end sections increases as \bar{n} is reduced at fixed M_w , G_N should fall off at small \bar{n} , as found in Figure 4. As this dilution effect is not included in current theories of ionomer dynamics (which assume long chains and many association sites per chain), a more quantitative analysis awaits further theoretical developments. At higher sulfonation levels than we have explored, where the end sections constitute an insignificant fraction of the total chain length, we would certainly anticipate the ionomers to show a higher G_N than does SEB147, but the very long relaxation times of highly functionalized ionomers make them impractical to study.

Further evidence for the importance of the relaxation of end sections comes from scrutiny of the G'' pseudomaster curves (Figure 5), corresponding to the G'

Table 3. WLF Constants^a for Unfunctionalized Terpolymers SEB16 and SEB28

polymer	c_1	c_2
SEB16	8.1	120.1
SEB28	8.6	128.2

^a Determined over 30–120 °C by fitting to $\log a_T = -c_1(T - T_{\text{ref}})/(c_2 + T - T_{\text{ref}})$, where $T_{\text{ref}} = 30$ °C.

pseudomaster curves in Figure 3 (and shifted according to the same a_T). For the ionomers, particularly those of lower functionalization level, there is a clear shoulder at high reduced frequencies (10^3 – 10^4 rad/s), which we identify with the relaxation of the polymer end sections. The position of this shoulder is similar to that of the loss peak in the unfunctionalized SEB precursors, indicating that the end sections relax at times comparable to t_d^0 . Though the end section constitutes only a fraction of the chain length, and thus might be expected to relax faster than t_d^0 , one of its ends is “pinned” at an ionic aggregate, since $\tau > t_d^0$ for these materials. Consequently, the end section must relax through retraction, a relatively slow process. A quantitative comparison is thwarted by the poor time–temperature superposition evident in Figure 5, which makes the reduced frequency at which this shoulder occurs correspondingly uncertain.

If indeed the shoulder in G'' (at 10^3 – 10^4 rad/s in Figure 5) arises from relaxation of the end sections, with little contribution from the ion-hopping (τ) and terminal (t_d) relaxations, then this relaxation should show the same temperature dependence as the unfunctionalized SEB terpolymers, which showed excellent superposition (see Figure 1) with shift factors a_T well-described by the Williams–Landel–Ferry (WLF) equation. Table 3 gives the parameters obtained by fitting the data for SEB16 and SEB28 separately to the WLF equation¹⁸ over 30–120 °C. These WLF constants were then used to calculate values of a_T for the corresponding ionomers, and these values used to construct the pseudomaster curves shown in Figure 6. For both sets of ionomers, these values of a_T succeed in superposing data in the region of the G'' shoulder (near 10^3 – 10^4 rad/s in Figure 6), confirming that the shoulder does indeed reflect the relaxation of nonionic portions of the chains, which we take here to be the end sections. Note also that the prominence of the shoulder is reduced as the functionalization level is increased (i.e., as the fraction of chain length occupied by the end sections decreases).

However, the data in Figure 6 show very poor superposition at low frequencies, since the ion-hopping and terminal relaxations active at low frequencies are characterized by different activation energies than the relaxation of the end segments. Close examination of Figure 6, especially Figure 6b, shows that the separation between the low-frequency peak (10^{-2} – 10^1 rad/s) and the high-frequency shoulder (10^3 – 10^4 rad/s) is progressively reduced as the temperature is increased; that is, the relaxations approach each other at higher temperatures. This indicates that the ion-hopping and terminal relaxations responsible for the low-frequency peak have higher activation energies than does the motion of the nonionic polymer chain, consistent with prior observations comparing the activation energies (obtained through TTS) for ionomers with their nonionic precursors.^{6,24,27}

C. Cation Diffusion. In their studies of SPS ionomers (which had $\bar{n} > 50$), Weiss et al.²⁷ observed a distinct peak in G'' , corresponding to the ion-hopping

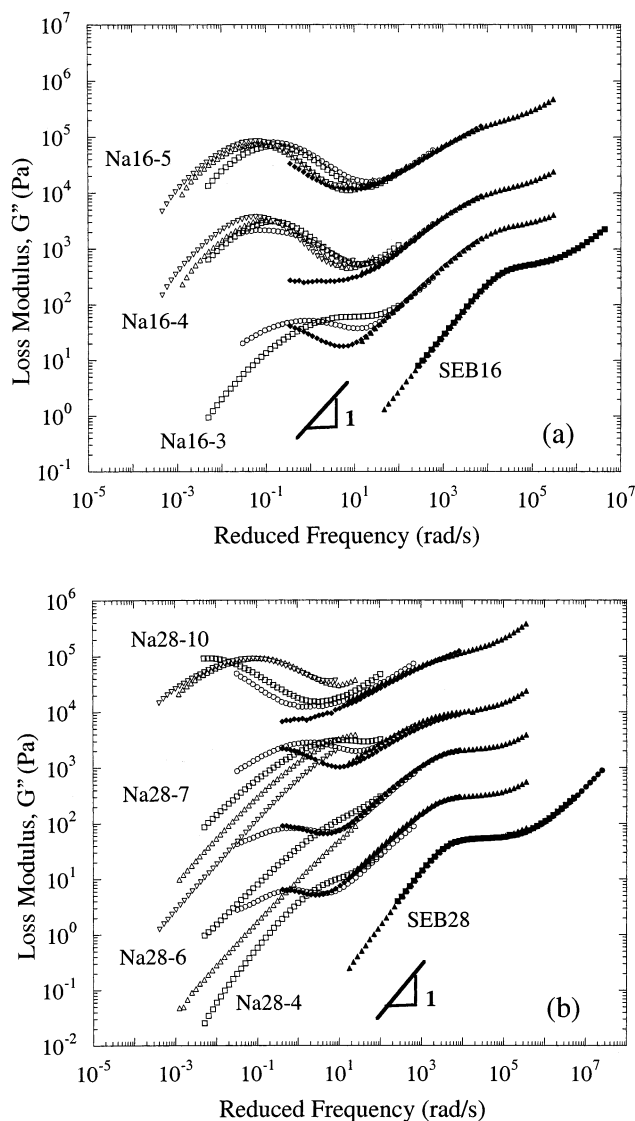


Figure 6. Loss modulus (G'') pseudomaster curves at 120 °C, constructed using shift factors calculated from the WLF fits to the unfunctionalized SEB precursors. The G'' data for the most highly functionalized ionomer in each panel are unshifted; the other curves are shifted downward by factors decreasing progressively with ion content, for clarity. Symbols and vertical shifts of curves are the same as in Figure 5.

relaxation. However, the analysis presented in the preceding section indicates that in our ionomers of modest \bar{n} the ion-hopping process (characteristic time $\tau > t_d^0$) overlaps with the terminal relaxation (t_d). A direct measurement of τ could confirm this conclusion. Previously, we have measured the diffusion coefficient of the ionic groups (\mathcal{D}_{ion}) in E/MAA ionomers using profile microanalysis.^{6,30,31} Briefly, films of ionomers differing only in the neutralizing cation (Na^+ vs Li^+ here) are laminated together to create a diffusion pair, which is then annealed for a given time and temperature. Subsequently, the laminate is cut in cross section, and the concentration profile of the cations through the laminate is determined with a scanning electron microscope employing energy-dispersive X-ray detection. The concentration profile is fit to the Fickian solution of the governing diffusion equation to extract \mathcal{D}_{ion} , which is related to τ through the characteristic interaggregate (“hop”) distance. Though we refer to “cation” diffusion here, since it is the concentration profile of the cations

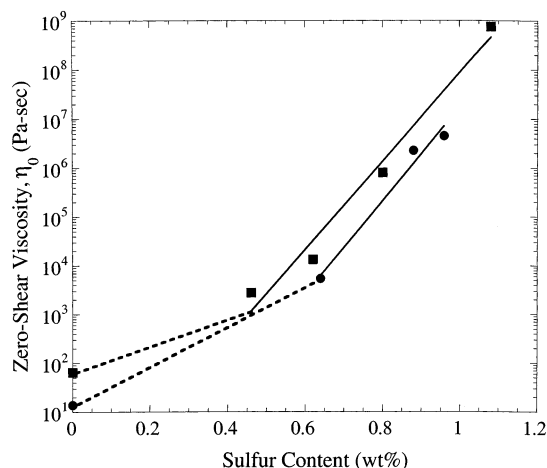


Figure 7. Zero-shear viscosity η_0 at 120 °C as a function of sulfur content for Na⁺ ionomers derived from SEB16 (●) and SEB28 (■). Solid lines correspond to the best exponential fits for the two sets of ionomers; dashed lines are guides to the eye, each connecting to the η_0 value for the corresponding unfunctionalized SEB precursor (at zero sulfur content).

which is actually measured, we emphasize that the ion-hopping mechanism presumes that the ions move as bound cation–anion pairs. However, within an aggregate, the cations should be able to rapidly exchange between different sulfonate groups, permitting a diffusive movement of the cations (through a series of hops with different anion “partners”) which greatly exceeds the rate of center-of-mass diffusion of the polymer chain.^{6,30}

We applied this same approach to our sulfonated SEB ionomers by preparing a complementary Li⁺-neutralized ionomer to serve as the outer layers of the laminate. Since the resolution limit of this electron probe analysis method is approximately 1 μm , specimens must be annealed under conditions that permit diffusion of the ionic groups over several microns (i.e., annealing for very many times τ). Unfortunately, since τ and t_d in our Na16 and Na28 SSEB ionomers are not separated by several orders of magnitude (as they are in the E/MAA ionomers we have studied by this method previously⁶), annealing for the necessary time also permits bulk flow of the material under its own weight, ruining the laminate. Since η_0 increases with molecular weight, but τ is presumably independent of the total polymer molecular weight (as it reflects the motions of individual chain sections which bear an ionic group), this problem can be ameliorated by using ionomers made from higher M_w SEB precursors. We found that satisfactory specimens for the diffusion experiments could be prepared from an SEB47 derivative (Na47-9 laminated between Li47-9 films), though this same ionomer did not exhibit terminal relaxation by rheometry over the accessible temperature and frequency window.

Diffusion measurements on the Na47-9/Li47-9 laminate yielded $\mathcal{D}_{\text{ion}} = 1.5 \pm 0.8 \times 10^{-12} \text{ cm}^2/\text{s}$ (uncertainty is ± 1 standard deviation between the data and the Fickian solution) at 120 °C. This value is more than an order of magnitude below the values of \mathcal{D}_{ion} which we have measured for E/MAA ionomers,⁶ reflecting stronger interionic associations in the present case. The ion-hopping time τ may be estimated from $\tau = d^2/\mathcal{D}_{\text{ion}}$, where d is the average distance between ionic aggregates. Unfortunately, small-angle X-ray scattering on these ionomers does not show a distinct peak; therefore, we

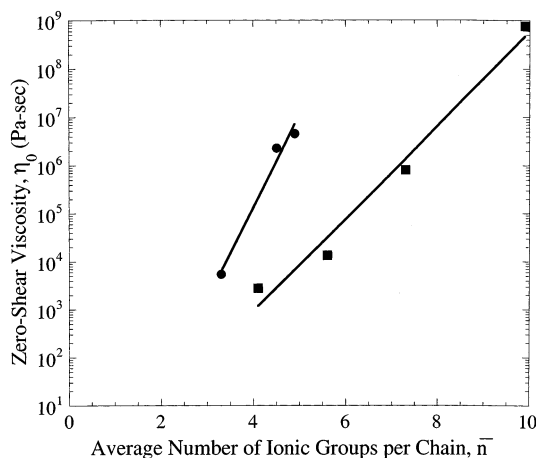


Figure 8. Zero-shear viscosity η_0 at 120 °C as a function of the average number of ionic groups per chain, \bar{n} , for Na⁺ ionomers derived from SEB16 (●) and SEB28 (■). Solid lines correspond to the best exponential fits for the two sets of ionomers.

approximate the distance between aggregates as 6 nm, from published data for sulfonated polystyrene ionomers at a similar ion content.³² This estimate yields $\tau = 0.2 \text{ s}$ at 120 °C, corresponding to a frequency of approximately 5 rad/s. This frequency, in turn, is consistent with the data for Na16 and Na28 ionomers in Figures 5 and 6, where 5 rad/s corresponds to the region of the major peak in G'' , on the high-frequency side.

D. Comparison with Theories of Ionomer Dynamics. We developed this sulfonated ionomer system with the goal of comparing the experimentally observed flow behavior to current theories of ionomer dynamics.^{2,8} But while the theories pertain to ionomers that are well-entangled and have a large number of ionic groups per chain, the strong associations between the ionic groups (i.e., long τ) in our sulfonated SEB ionomers limits us to only a few ionic groups per chain and modest molecular weights before t_d becomes unmanageably long. Despite this restriction, some comparisons are both possible and informative. Figure 7 presents values of η_0 at 120 °C for the Na16 and Na28 ionomers, extrapolated from the dynamic shear experiments, plotted against sulfur content (a measure of the ion content; 1 wt % sulfur corresponds to an equivalent weight (EW) of 3200 g ionomer/mol SO₃, with sulfur content and EW reciprocally related). While η_0 is seen to depend on both M_w and ion content, the dependence on M_w is relatively weak; indeed, the curves for the Na16 and Na28 ionomers seem to be displaced by an essentially constant factor. This result suggests that η_0 depends on the number *density* of ionic groups in the material, not simply on the average number of ionic groups per chain, \bar{n} (which is proportional to *both* M_w and ion content). Sticky reptation theory⁶ predicts that $\eta_0 \sim \bar{n}^2 M^{3/2} \tau$, such that plots of $\log(\eta_0)$ vs \bar{n} for the Na16 and Na28 ionomers should have a common slope, simply offset by a factor of $(28/16)^{3/2} = 2.3$. Figure 8 demonstrates that this is clearly *not* observed for our sulfonated SEB ionomers, and extrapolation of the best-fit lines indicates that the viscosity ratio of 2.3 would be achieved only for $\bar{n} < 2$, a region where the theory's expectation of many ionic groups per chain is clearly unmet. Moreover, both of the data sets in Figure 8, if force-fit to power laws in η_0 vs \bar{n} , have apparent power-law slopes (14–18) far in excess of the expected value of 2.

We conclude that this disparity reflects a strong dependence of τ on the ion content (number density of ionic groups), with τ becoming longer as the material is more heavily functionalized. This could arise, for example, from tighter binding³⁰ of individual ionic groups into the larger aggregates³³ formed at higher functionalization levels. In fact, for SPS ionomers, Weiss et al.²⁷ observed that the G'' peak corresponding to the ion-hopping relaxation shifted nearly 4 orders of magnitude to lower frequency as the sulfonation level increased from 1.8 to 5.8 mol %. However, the inaccessibly long terminal times of those SPS ionomers precluded an assessment of how this shift in τ was reflected in t_d or η_0 . The data of Figure 7 reveal a dominant influence of ion content (as opposed to \bar{n}) on t_d : over the range common to both Na16 and Na28 ionomers (0.6–1.0 wt % sulfur; EW 3200–5300 g of ionomer/mol of SO_3), η_0 increases by a factor of 10^3 , while \bar{n}^2 increases by less than a factor of 3. A potentially strong dependence of τ on ion content should be borne in mind when interpreting rheological data for any random ionomer.

Conclusions

Model ionomers of narrow molecular weight distribution, linear architecture, controllable and variable functionalization levels, and low glass transition temperature (15 °C) were synthesized via anionic polymerization of styrene and butadiene in the presence of TMEDA, followed by catalytic hydrogenation, sulfonation with acetyl sulfate, and neutralization. Melt rheological measurements of these sulfonated SEB ionomers neutralized with tributylamine demonstrated the absence of major backbone rearrangements due to the sulfonation reaction. Linear viscoelastic measurements on these ionomers revealed the presence of multiple relaxation mechanisms as peaks in G'' . Moreover, the linear viscoelastic material functions depart substantially from time–temperature superposition, indicating that the underlying mechanisms follow different temperature dependences.

All the ionomers exhibit a relaxation at the high-frequency end of the rubbery plateau, which we identify with relaxation of the “end sections” of the chain: the portions of the chain lying between the chain ends and the ionic group closest to each chain end. Rapid relaxation of these end sections leads to a dynamic dilution of the network, as most of the junctions in the network are formed by entanglements rather than by ionic crosslinks. The low-frequency end of the rubbery plateau is bounded by the relaxation of the ionic associations. However, at the low molecular weights and small number of ionic groups per chain characteristic of our ionomers, a second rubbery plateau characteristic of the entanglement network is not observed at lower frequencies. Instead, at frequencies below the reciprocal of τ , we see a gradual transition to terminal behavior, indicating that the ion-hopping and terminal relaxations overlap strongly. The failure of time–temperature superposition observed here is thus not principally due to differences in activation energy between the ion-hopping and terminal processes, but rather to the difference between the activation energies for these two processes and that for relaxation of the chains’ nonionic end sections.

Finally, we observe an extremely strong dependence of the terminal relaxation time on the average number of ionic groups per chain (\bar{n}), much stronger than the

\bar{n}^2 dependence anticipated by current theories of ionomer dynamics. This deviation results from the strong dependence found for τ on ion content (number density of ionic groups), which we expect is a general phenomenon at typical ion contents.

Acknowledgment. Financial support for this project was provided by DuPont Packaging & Industrial Polymers and by the donors of the Petroleum Research Fund, administered by the American Chemical Society (30658-AC7). The authors thank Dr. Adel Halasa of the Goodyear Tire & Rubber Co. for performing the ozonolysis experiments to determine the degree of randomness in these SBR copolymers and Brian K. Hamilton for invaluable assistance with the light scattering measurements.

References and Notes

- (1) Register, R. A.; Prud'homme, R. K. In *Ionomers: Synthesis, Structure, Properties and Applications*; Tant, M. R., Mauritz, K. A., Wilkes, G. L., Eds.; Chapman & Hall: New York, 1997; p 208.
- (2) Colby, R. H.; Zheng, X.; Rafailovich, M. H.; Sokolov, J.; Peiffer, D. G.; Schwarz, S. A.; Strzhemechny, Y.; Nguyen, D. *Phys. Rev. Lett.* **1998**, *81*, 3876.
- (3) Cooper, W. *J. Polym. Sci.* **1958**, *28*, 195.
- (4) Hara, M.; Eisenberg, A.; Storey, R. F.; Kennedy, J. P. In *Coulombic Interactions in Macromolecular Systems*; ACS Symp. Ser. 302; Eisenberg, A., Bailey, F. E., Eds.; American Chemical Society: Washington, DC, 1986; p 176.
- (5) Longworth, R. In *Ionic Polymers*; Holliday, L., Ed.; John Wiley & Sons: New York, 1975; p 69.
- (6) Tierney, N. K.; Register, R. A. *Macromolecules* **2002**, *35*, 2358.
- (7) Makowski, H. S.; Lundberg, R. D.; Singhal, G. S. U.S. Patent 3,870,841, issued March 11, 1975, to Exxon Research and Engineering Co.
- (8) Leibler, L.; Rubinstein, M.; Colby, R. H. *Macromolecules* **1991**, *24*, 4701.
- (9) Antkowiak, T. A.; Oberster, A. E.; Halasa, A. F.; Tate, D. P. *J. Polym. Sci., Part A1* **1972**, *10*, 1319.
- (10) Chang, C. C.; Halasa, A. F.; Miller, J. W.; Hsu, W. L. *Polym. Int.* **1994**, *33*, 151.
- (11) Hahn, S. F. *J. Polym. Sci., Part A: Polym. Chem.* **1992**, *30*, 397.
- (12) Adams, J. L.; Quiram, D. J.; Graessley, W. W.; Register, R. A.; Marchand, G. R. *Macromolecules* **1998**, *31*, 201.
- (13) Storey, R. F.; George, S. E.; Nelson, M. E. *Macromolecules* **1991**, *24*, 2920.
- (14) Register, R. A.; Bell, T. R. *J. Polym. Sci., Part B: Polym. Phys.* **1992**, *30*, 569.
- (15) Loo, Y.-L. Ph.D. Thesis, Princeton University, 2001.
- (16) Sebastian, J. M.; Register, R. A. *J. Appl. Polym. Sci.* **2001**, *82*, 2056.
- (17) Tierney, N. K. Ph.D. Thesis, Princeton University, 2001.
- (18) Ferry, J. D. *Viscoelastic Properties of Polymers*, 3rd ed.; John Wiley and Sons: New York, 1980.
- (19) Richardson, M. J.; Savill, N. G. *Polymer* **1977**, *18*, 3.
- (20) Krishnamoorti, R. Ph.D. Thesis, Princeton University, 1994.
- (21) Siebourg, W.; Lundberg, R. D.; Lenz, R. W. *Macromolecules* **1980**, *13*, 1013.
- (22) Weiss, R. A.; Agarwal, P. K.; Lundberg, R. D. *J. Appl. Polym. Sci.* **1984**, *29*, 2719.
- (23) Weiss, R. A.; Stamato, H. *Polym. Eng. Sci.* **1989**, *29*, 134.
- (24) Earnest, T. R., Jr.; MacKnight, W. J. *J. Polym. Sci., Polym. Phys. Ed.* **1978**, *16*, 143.
- (25) Eisenberg, A.; Navratil, M. *Polym. Lett.* **1972**, *10*, 537.
- (26) Vanhoorne, P.; Register, R. A. *Macromolecules* **1996**, *29*, 598.
- (27) Weiss, R. A.; Fitzgerald, J. J.; Kim, D. *Macromolecules* **1991**, *24*, 1071.
- (28) Milner, S. T.; McLeish, T. C. B.; Young, R. N.; Hakiki, A.; Johnson, J. M. *Macromolecules* **1998**, *31*, 9345.
- (29) McLeish, T. C. B.; Milner, S. T. *Adv. Polym. Sci.* **1999**, *43*, 195.
- (30) Tierney, N. K.; Register, R. A. *Macromolecules* **2002**, *35*, 6284.
- (31) Tierney, N. K.; Register, R. A. *J. Mater. Res.* **2002**, *17*, 2736.
- (32) Yarusso, D. J.; Cooper, S. L. *Macromolecules* **1983**, *16*, 1871.
- (33) Tomita, H.; Register, R. A. *Macromolecules* **1993**, *26*, 2791.